

## Article

# Exceptional In Situ Preservation of Chondrocranial Elements in a Coniacian Mosasaurid from Colombia

María Eurídice Páramo-Fonseca <sup>1,2,\*</sup> , José Alejandro Narváez-Rincón <sup>1,2</sup>, Cristian David Benavides-Cabra <sup>1,2</sup> and Christian Felipe Yanez-Leaño <sup>3</sup>

<sup>1</sup> Departamento de Geociencias, Universidad Nacional de Colombia, Bogotá 111321, Colombia; janarvaezr@unal.edu.co (J.A.N.-R.); cdbenavidesc@unal.edu.co (C.D.B.-C.)

<sup>2</sup> Museo Geológico Nacional José Royo y Gómez, Servicio Geológico Colombiano, Bogotá 111321, Colombia

<sup>3</sup> Grupo de Investigación Clínica SHAI0, Fundación Clínica SHAI0, Bogotá 111121, Colombia; christian.yanez@shai0.org

\* Correspondence: meparamof@unal.edu.co

**Abstract:** The first record of well-preserved chondrocranial elements in mosasaurids is here described. These elements are preserved in situ in a Coniacian skull found in north-central Colombia, inside a calcareous concretion. Based on a 3D model generated from computed tomography scans, we identified elements of the nasal and orbitotemporal regions. Our descriptions show that in this specimen, the chondrocranium was reduced, more so than in most lacertilians (including their closest recent relatives, the varanids), but not as severely as in snakes or amphisbaenians (which have an extremely reduced chondrocranium and limbs). The new evidence suggests that the reduction in the chondrocranium in mosasaurids could be related to modification of their limbs when adapting to aquatic environments, but also that in mosasaurids, the olfactory tract was reduced, and the optic muscle insertions occurred mainly in the interorbital septum. The exceptional preservation of the chondrocranial elements in the specimen is facilitated by a gray mineralization covering them. XRD analysis and thin section observations indicated that this mineralization is composed of microcrystalline quartz and calcite. We infer that this material was produced by a partial silicification process promoted by lower pH microenvironments associated with bacterial breakdown of non-biomineralized tissues during early diagenesis.

**Keywords:** mosasaurid; chondrocranium; Coniacian; Colombia



**Citation:** Páramo-Fonseca, M.E.; Narváez-Rincón, J.A.; Benavides-Cabra, C.D.; Yanez-Leaño, C.F. Exceptional In Situ Preservation of Chondrocranial Elements in a Coniacian Mosasaurid from Colombia. *Diversity* **2024**, *16*, 285. <https://doi.org/10.3390/d16050285>

Academic Editor: Nathalie Bardet

Received: 30 March 2024

Revised: 6 May 2024

Accepted: 7 May 2024

Published: 10 May 2024



**Copyright:** © 2024 by the authors. Licensee MDPI, Basel, Switzerland. This article is an open access article distributed under the terms and conditions of the Creative Commons Attribution (CC BY) license (<https://creativecommons.org/licenses/by/4.0/>).

## 1. Introduction

The chondrocranium is the cartilaginous portion of the vertebrate braincase [1–3]. Among gnathostomes, the chondrocranium has six recognizable components during development [2,3]: the nasal capsules, which support the nasal apparatus and may form the ethmoid plate; the orbital cartilages, located medial to the eyes; the otic capsules, which contain the inner ear; the parachordals, which form the posterior base of the braincase; a pair of rod-like trabeculae cranii that sit between the parachordals and the nasal capsules beneath the orbital cartilage and the interorbital septum; and the occipital and preoccipital arches, which enclose the posterior part of the brain. The trabeculae cranii eventually meet in the midline anteriorly to form the internasal septum [2,3], which ossifies to constitute the ethmoid and sphenethmoid bones [4]. The parachordals give rise to the basal plate, which ossifies to constitute the basioccipital-basisphenoid region of the skull [4]. The otic capsules ossify to form the prootic, opisthotic, and epiotic, and the occipital arch ossifies to form the supraoccipital and the exoccipitals [4] (Figure 1A). The nasal and orbital cartilages remain cartilaginous in adulthood [4]. The chondrocranium varies greatly among taxa regarding its frame-like structure, mineralization, and when and to what extent it is replaced by bone during ontogeny [1,3]. In reptiles, the grade of ossification and chondrification varies greatly [5]. In this group of vertebrates, the adult chondrocranium is divided into three

regions: the nasal, the orbitotemporal, and the otic-occipital region [2,6–9]. Anteriorly, the nasal region is formed by the nasal capsules, which are separated by the nasal septum, and posteriorly, it is formed by the planum antorbitale [9]. The orbitotemporal region is formed by the interorbital septum, the planum suprasedale, and the taeniae and pila chondrified in diverse degrees [9]. The otic and occipital regions are formed by the otic capsules and the basal plate [9].

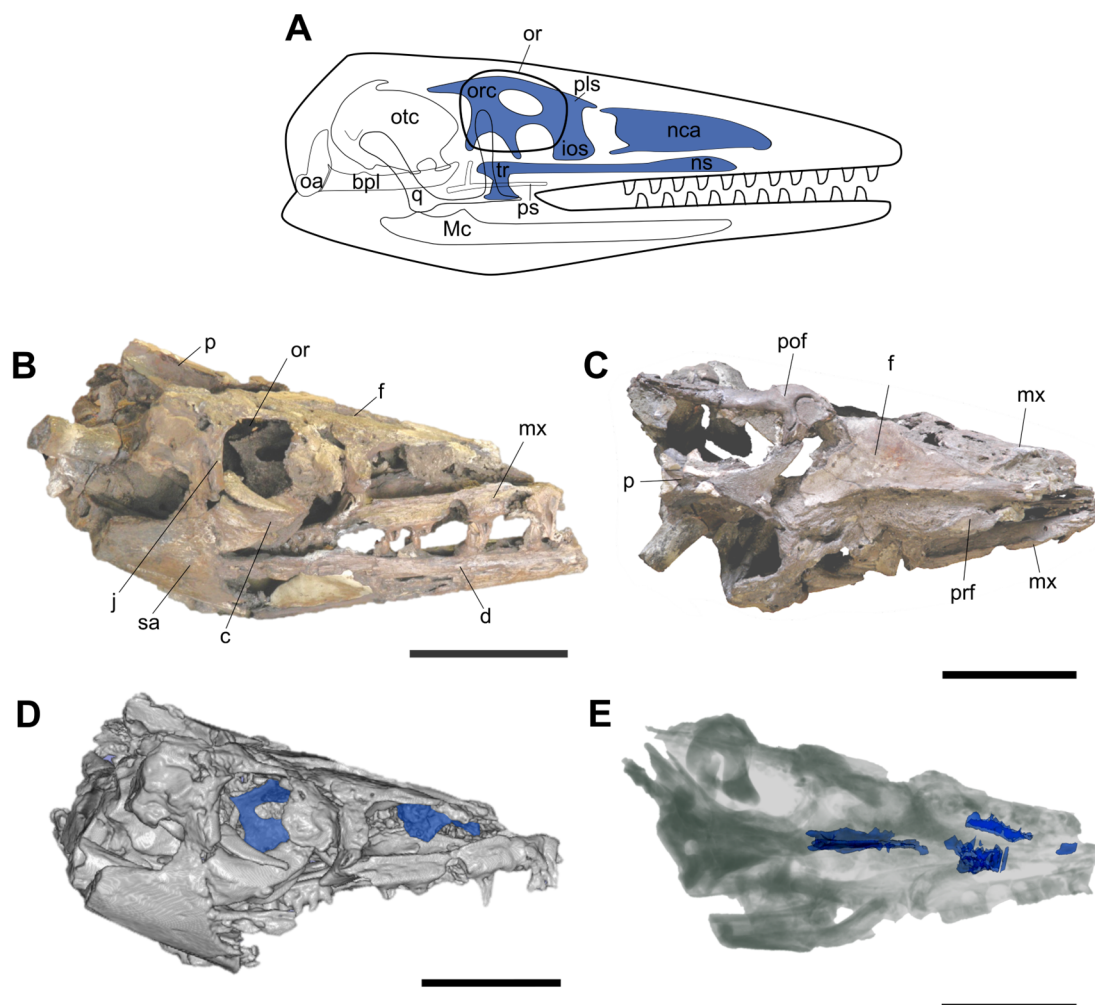


**Figure 1.** (A) Schematic diagram of a lizard-like chondrocranium in right lateral view (redrawn and modified from [2,3]) adapted to a mosasaur-like skull silhouette. (B–E) IGMp879524 skull showing the preserved in situ chondrocranial elements. (B,C) Photographs of the skull in (B), right lateral and (C) dorsal views. (D) Opaque 3D model of the skull in right lateral view (3D Slicer option CT-AAA). (E) Transparent 3D model of the skull in dorsal view (3D Slicer option CT-X-ray). The preserved chondrocranial elements are highlighted in blue. Part of the mandible and the braincase are not included in the 3D model. **Abbreviations:** bpl, basal plate; c, coronoid; d, dentary; f, frontal; ios, interorbital septum; j, jugal; Mc, Meckel's cartilage; mx, maxilla; nca, nasal capsules; ns, nasal septum; oa, occipital arch; or, orbit; orc, orbital cartilage; otc, otic capsule; p, parietal; pof, postorbitofrontal; prf, prefrontal; pls, planum suprasedale; ps, parasphenoid; q, quadrate; sa, surangular; tr, trabeculae cranii. Scale bars: 100 mm.

In lepidosaurs, a significant portion of the chondrocranium is generally retained into adulthood [3]. In most adult lepidosaurs, the nasal capsules, a nasal septum, an interorbital septum, and a central framework of slender bars (taeniae and pila) are retained [3]. In some lizards, parts of the taenia medialis and pila metoptica ossify, forming the orbitosphenoid [2].

In mosasaurs (Late Cretaceous marine lepidosaurs), the chondrocranium is almost unknown. Camp [10] described an orbitosphenoid in a *Plotosaurus* (*Kolposaurus*) skull from the Maastrichtian (Upper Cretaceous) of California. According to this author, the orbitosphenoid encloses the optic chiasma and provides support to the ventrolateral wall of the cerebrum. Additionally, Camp [10] described a brownish stain accompanied by bone granules and identified it as a partially preserved interorbital septum anterior to the orbitosphenoid. Bellairs [5], based on descriptions of the chondrocranium development in sauropsids, including varanids, stated that the partially interorbital septum identified by [10] might be called septosphenoid. In some specimens of *Platecarpus* and one of *Mosasaurus*, a bone with a similar form of the orbitosphenoid of *Plotosaurus* has been interpreted as orbitosphenoid [11].

Another mosasaurid specimen preserving chondrocranial elements was reported by [12]. It consists of a skull (IGMp879524), reported by [12] under the catalog number IPN-2, preserving in situ an almost complete chondrocranium. The specimen was found in Coniacian beds from north-central Colombia and constitutes the first record of well-preserved chondrocranial elements in a mosasaurid. The osteo-anatomic description and the taxonomic determination of the specimen is currently under publication. In this contribution, we fully describe and identify the preserved chondrocranial elements of this specimen, discuss the probable functional implications of their anatomy, and comment on their preservation features.

## 2. Materials and Methods

The specimen (IGMp879524) is housed in the paleontological collection of the Museo Geológico Nacional José Royo y Gómez at the Servicio Geológico Colombiano (SGC). It consists of a good portion of an articulated three-dimensionally preserved skull, lacking its anterior end, and maintaining some delicate intracranial structures, such as chondrocranial elements (Figure 1A,B). It was found in a calcareous concretion from Coniacian beds [12] of the Galembó Formation [13], a geologic unit formerly known as the Galembó Member of the La Luna Formation [14]. The specimen was collected in the surroundings of the Lebrija municipality, Santander department, northern Colombia [12].

The preparation of IGMp879524 was mainly performed chemically, with an initial mechanical treatment. The chemical preparation revealed the presence of a gray mineralization, indissoluble in acid, which was found coating a large part of the bone surfaces and forming some laminae in the concretion matrix. This material was also found firmly adhered to intracranial thin and delicate bones and cartilages, as the chondrocranium components. In these cases, we preserve the coverage without subjecting the specimen to mechanical preparation to avoid compromising the integrity of the fossilized bones or cartilages. The position of some bones of the skull, as the quadrates, which are displaced and rotated dorsally into the temporal fenestrae, suggests that the skull was deposited upside down. This is important because a few delicate detached fragments found on the ventral surface of the frontal could correspond to separated elements from the chondrocranium that fell upon the internal surface of the frontal.

To describe and identify the chondrocranial elements of the skull (IGMp879524), we built a 3D model from computed X-ray tomography (CT) scans of the specimen (Figure 1C,D). Most of the mandibles and some fragments of the occipital region, which are separated from the main skull piece, were not joined for scanning given the fragility of these elements. The CT scan was performed at the Clínica SHAIÓ, Bogotá, Colombia, using a Canon Aquilon One with a precision of 0.5 mm, KVP: 120, head protocol, and bone filter. The final voxel size was 0.25 mm. A 3D model was made using the open-source software 3D Slicer 5.2.2. The identification of the chondrocranial elements follows [5–7]. We adopted the terminology used by these authors in their description of the development of the chondrocranium in squamate reptiles.

To evaluate the composition of the gray mineralization, we performed an X-ray diffraction (XRD) analysis of a sample of this material recovered from the concretion. Also, to

contrast the matrix and the gray mineralization composition, we made observations on three thin sections: one of the calcareous matrix with bone, one of the gray mineralization, and one including both the mineralization and the calcareous matrix. The XRD analysis was performed at the Litho-geochemical Characterization Laboratory of the Departamento de Geociencias of the Universidad Nacional de Colombia. The sample was prepared for the XRD analysis following the parameters established by [15,16]. The measurements were taken using a Bruker Co. Karlsruhe, Germany D2 PHASER with a copper lamp, and the results were interpreted using the software Diffract.EVA.V4.2.1. The thin sections were made at the Petrographic Techniques Laboratory of the Departamento de Geociencias of the Universidad Nacional de Colombia. All the figures in this contribution were assembled using the open-source software Inkscape 1.3.2.

### 3. Anatomical Description

Based on direct observations on the fossil, as well as on the CT scan slices and 3D model, we identified the following chondrocranial elements (see Figures 2 and 3): some poorly preserved nasal elements, which probably represent remains of the nasal capsules and fragments of the nasal septum; orbitotemporal elements, including well-preserved planum suprasettale and interorbital septum with the posterior septal fenestra, the taenia medialis, the cartilago hypochiasmatica, and the trabecula communis. All these elements were preserved covered by a gray mineralization. Nevertheless, the surfaces of these elements, mainly the interorbital septum, show a porous texture, indicating a cartilaginous origin (Figure 2F).

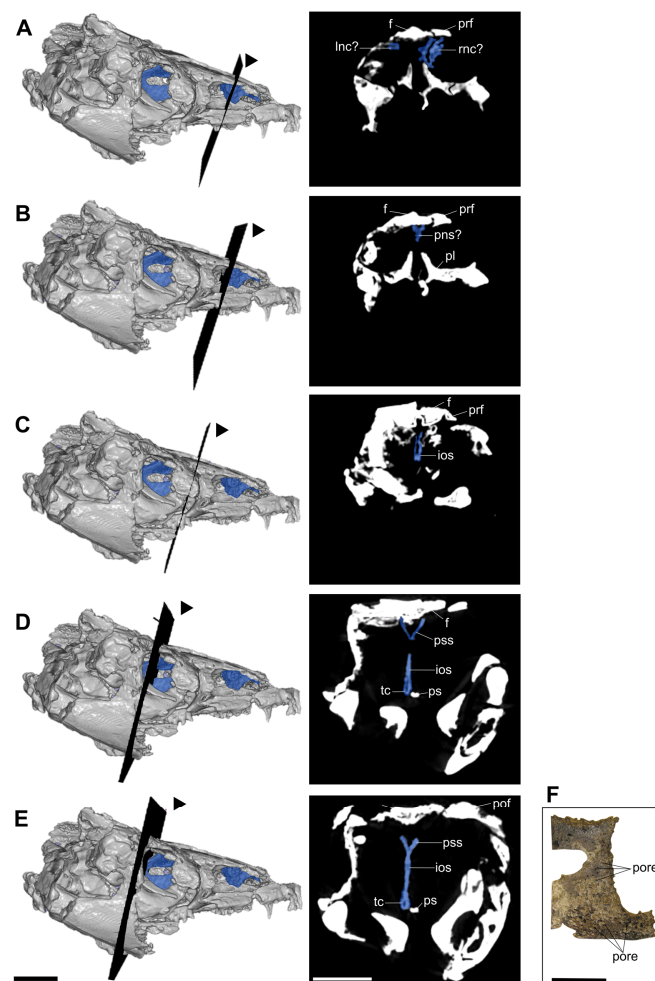


**Figure 2.** Location of the chondrocranial elements in IGMp879524 skull. (A–E) Three-dimensional model (left) and cross-section scans (right) of the skull without the complete mandible. The chondrocranial

elements are highlighted in blue. The black planes and arrows in the 3D models indicate the position and orientation of the cross-sections shown on the right side. (F) Detail of the interorbital septum in its left side showing its porous texture. **Abbreviations:** *f*, frontal; *ios*, interorbital septum; *lnc?*, probable element of the left nasal capsule; *pl*, palatine; *pns?*, probable element of the posterior region of the nasal septum; *pof*, postorbitofrontal; *prf*, prefrontal; *ps*, parasphenoid rostrum; *pss*, planum suprasedale; *rnc?*, probable element of the right nasal capsule; *tc*, trabeculae comunis. Scale bars: (A–E) 50 mm; (F) 30 mm.

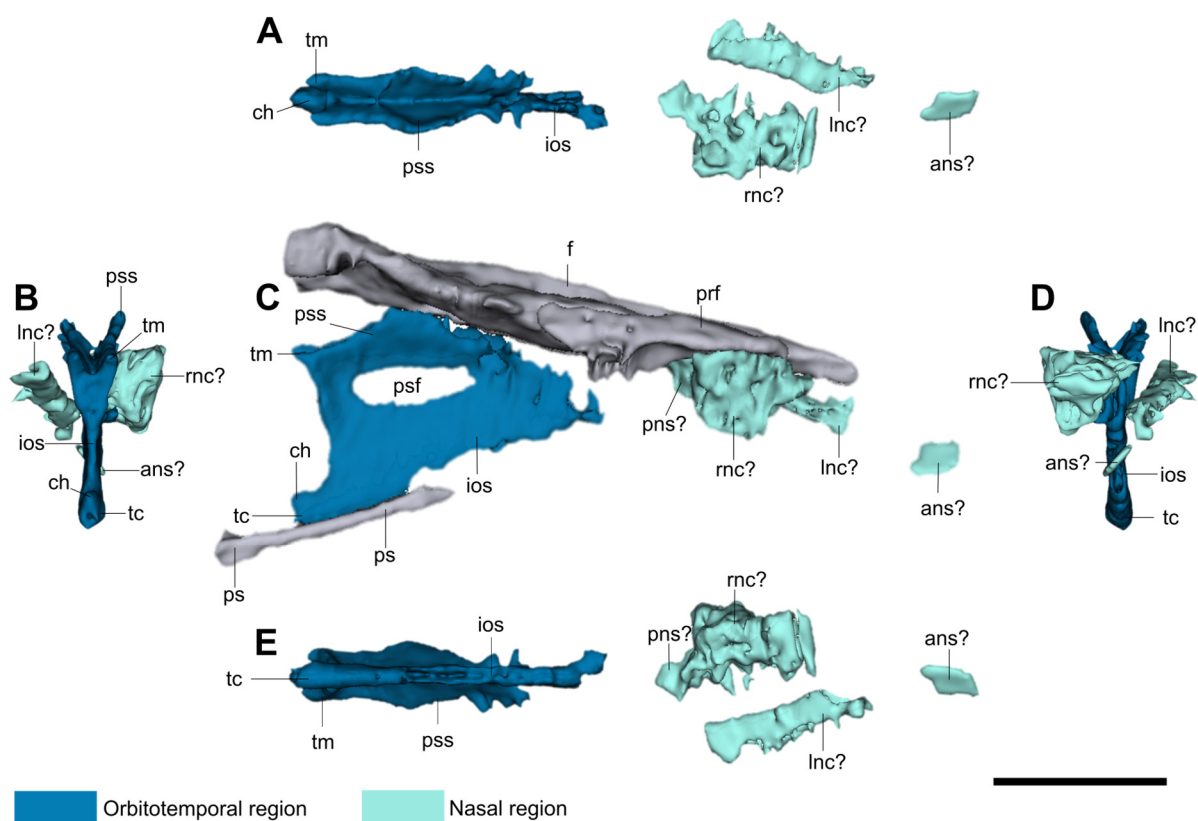


**Figure 3.** Three-dimensional model of the chondrocranial elements and contacting bones of IGMp879524 in (A) dorsal, (B) posterior, (C) right lateral, (D) anterior, and (E) ventral views. **Abbreviations:** *ans?*, probable element of the anterior region of the nasal septum; *ch*, cartilago hypochiasmatica; *f*, frontal; *ios*, interorbital septum; *lnc?*, probable element of the left nasal capsule; *pns?*, probable element of the posterior region of the nasal septum; *prf*, prefrontal; *ps*, parasphenoid rostrum; *psf*, posterior septal fenestra; *psr*, parasphenoid rostrum; *pss*, planum suprasedale; *rnc?*, probable element of the right nasal capsule; *tc*, trabeculae comunis; *tm*, taenia medialis. Scale bar: 50 mm.

### 3.1. Nasal Region

We recognize three chondrocranial structures preserved in the nasal region. Anteriorly, there are two irregular bulbous masses, one on each side of the sagittal plane, contacting the prefrontals (Figures 2A and 3C). The right one, the best preserved, increases its size anteroventrally reaching the palatine. It has an internal narrow canal, almost vertical in cross-section (Figure 2A). The left mass seems incomplete; it is dorsoventrally compressed and slightly inclined anteroventrally and shows an internal space, but in this case, it is a narrow subhorizontal canal (Figure 2A). According to the *Varanus* cross-sections presented by [17], the canals of these two structures in IGMp879524 could represent the olfactory chambers for the nasal sacs, since they are located between frontal and palatine. However, in this same anatomical position, Konishi [18] proposes the presence of salt-glands in a halisaurine mosasaur. The third structure, a probable element of the nasal septum, is located

posterior to the described masses and is a mid-sagittal structure that dorsally contacts the anterior end of the frontal internarial bar (Figure 2B). This structure is posteriorly short and subreniform in cross-section, and anteriorly it increases in height and becomes subtriangular in cross-section, pointing ventrally and with a small canal located in the dorsal midline (Figure 2B).

The preserved nasal elements, as well as the presence of a narrow canal in the lateral masses, are reminiscent of the morphology of the nasal septum and nasal capsules described by [7,9,17]. However, the poor preservation of these structures prevents us from confidently affirming their identification as the nasal septum and capsules.

### 3.2. Orbitotemporal Region

In the orbitotemporal region, the interorbital septum, the planum suprasedale, the taeniae medialis, the trabecula communis, and the cartilago hypochiasmatica are preserved in situ. The taenia marginalis is completely absent on both sides of the skull, and no pilae are preserved in situ. However, since the skull was deposited in an upside-down position, a few small fragments of flattened rod-like structures laying on the ventral surface of the frontal, at the level of the anterior interorbital septum and near both displaced epipterygoids, could be interpreted as broken fragments from both pilae metoptica that have become detached by the thrust of the falling epipterygoids. No orbitosphenoids were identified among these fragments. Considering the symmetric absence of the taeniae marginalis, and the presence of the gray mineralized coverage in all other anterior and posterior intracranial elements, we consider that the absence of these elements is not due to preservation effects; instead, it is because they were not originally present.

The interorbital septum is the main element preserved in the orbitotemporal region. It is a thin mid-sagittal plate dividing both orbits (Figure 2D,E). It is anteriorly reduced and does not contact the nasal elements of the chondrocranium (Figure 3). The interorbital septum, together with the planum suprasedale, form a Y-shaped structure in vertical cross-section (Figures 2E and 3B). Ventrally, the interorbital septum thickens in the trabecula communis (Figures 2E and 3B,D) and reaches the slender anterior rostrum (cultriform process) of the parasphenoid. Due to taphonomic processes, the interorbital septum does not coincide exactly with the parasphenoid rostrum in the sagittal plane (Figure 2C,D). The interorbital septum is perforated on its upper half by a large oval foramen (Figure 3C), which is recognized as the posterior septal fenestra (following [7]).

The planum suprasedale is formed by two short latero-dorsally directed ala-like plates, which form a dorsal angled concavity (Figure 2D,E). It extends anteroposteriorly in two different planes. Anteriorly, the planum suprasedale is horizontal or parallel to the ventral surface of the frontal, whereas posteriorly it is inclined, separating it from the skull roof (Figure 3C). The planum suprasedale ventrally connects to the interorbital septum and forms a portion of the dorsal margin of the posterior septal fenestra (Figures 2D and 3C). Dorsally, in its horizontal portion, the planum suprasedale reaches the frontal, just where the anterior end of the cerebral hemispheres and the olfactory canal are located on the ventral surface of the frontal.

The trabecula communis forms a wedge-shaped thickening of the ventral border of the interorbital septum (Figure 2D,E). It shortly projects posteriorly from the posteroventral margin of the interorbital septum (Figure 3). Above this short projection of the trabecula communis there is a small bulge directed dorsally that could be identified as the cartilago hypochiasmatica (Figure 3C). The taeniae medialis are represented by two short bars projected posterodorsally from the posterior ends of the planum suprasedale (Figure 3). The posterior margin of the interorbital septum, the ventral margin of the taenia medialis, and the preserved dorsal margin of the cartilago hypochiasmatica should have formed the anterior and part of the dorsal and ventral margins of the optic fenestra, as has been illustrated for most lacertilians [2,5,7].

#### 4. Functional Implications

The chondrocranium in IGMp879524 is comparable to that of nearly all described extant lepidosaurs [2,5,9,19–21]; it has similar components arranged in the nasal and orbitotemporal regions. This condition, previously unknown in mosasaurids, allows us to project some of the morphofunctional studies carried out on the chondrocranium of recent lepidosaurs, towards the functionality of the chondrocranium in mosasaurids.

In the studied specimen (IGMp879524), the nasal region, although poorly preserved, allows us to affirm that the chondrification of the internasal septum was very reduced. The orbitotemporal region is also reduced; the planum suprasedale is narrow even though the skull is wide; it is not laterally expanded, differing from most other lizards [5,22]; the pilae are completely absent, except for probable detached fragments of the pila metóptica, and from the taeniae, only a reduced taenia medialis is present. Following the parameters used by [22] to evaluate the reduction degree of the chondrocranium in lepidosaurs, this condition shows that the orbitotemporal region of the chondrocranium of IGMp879524 is reduced, although not extremely reduced. According to these features, some functional implications can be analyzed.

Following the anatomical description of the chondrocranium of some lizards presented by [2,22], the planum suprasedale supports the olfactory tract dorsally, and posterodorsally it supports parts of the telencephalon and diencephalon. The reduced planum suprasedale contacting the frontal in IGMp879524 forms a narrow cavity for the olfactory tract, suggesting this tract was slender in this specimen. In addition, Bellairs [2] and Jones et al. [20] show that in most lizards, behind the posteroventral border of the interorbital septum, the optic nerves (nerve II) enter the brain (optic chiasma), delimited posteriorly by the pila metoptica on each side, and dorsally by the taenia medialis on each side of the interorbital septum. In IGMp879524, each of the taenia medialis and pila metoptica, forming the foramen for the optic nerve, seems greatly reduced, suggesting a narrow foramen for these nerves.

Although it has been proposed that the structural variation of the chondrocranium in squamates could have functional implications in skull mechanics, its biomechanical role in vertebrates remains poorly understood [20]. Jones et al. [3] found no evidence to support a vertical strut role for the chondrocranium in adult lizards. In contrast, according to [3], the role of the chondrocranium is more evident in an adequate growth of the skull during the embryologic development. Jones et al. [20], modeling the responses of strains on the chondrocranium of a lizard (*Salvator merianae*), shows that the chondrocranium only helps to dampen the load on the cranial bones from the stresses generated by the tensions and compressions when biting. These observations could indicate that in mosasaurids, as in most vertebrates, the chondrocranium played an important role during the embryologic development, to obtain an undeformed cranial morphology in the adult. They also indicate that, in the adult stage, the chondrocranium helped to dampen the loads on the cranial bones when biting, as well as to protect the olfactory tract and support muscles and other soft tissues.

According to [21], in the embryos of *Tuatara punctatus*, there are some muscles for moving the eye that are inserted mainly into the interorbital septum, but also into the planum suprasedale and the pila metoptica. The latter is highly fused with the pila antotica and pila accesoria, forming a continuous plate in *T. punctatus*. This shows the great importance of these parts of the chondrocranium in the proper functioning of the eye. The well-preserved interorbital septum and the absence of a fused pilae plate in IGMp879524 suggest that the optic muscle insertions in this mosasaur occurred mainly in the interorbital septum.

Yaryhin et al. [22] suggested that the reduction in the chondrocranial elements could be related to modifications on the appendicular skeleton. These authors show how in lepidosaurs with reduced limbs, there is a tendency for the chondrocranium to shrink. Mosasaurs had not been analyzed in this aspect because of the lack of information on their chondrocranium. Our description provides for the first-time reliable information on the chondrocranium of mosasaurs and shows that, in these aquatic lizards, the chondrocranium

was reduced, more than in most lacertilians, including their closest recent relatives, the varanids, but not as much as in snakes or amphisbaenians, which have an extreme reduction in their chondrocranium and their limbs [22]. The reduced chondrocranium of IGMp879524 constitutes a new datum for future analyses. Although much information is still lacking, the reduction in the chondrocranium in our specimen allows us to suggest that a reduction in the chondrocranium in mosasaurs could be related to the modification of their limbs for adaptation to an aquatic life.

### 5. Preservation

The specimen IGMp879524 is preserved in a concretion (nodule) found in a limestone sequence of the Galembó Formation. The skull has a gray mineralization that is indissoluble in formic acid, firmly adhered, and covering a large part of the bone surfaces and all preserved chondrocranium elements (Figure 4A,B). This mineralization is also present in the concretion matrix as irregular laminae (Figure 4A,B). The XDR analysis performed on this gray mineralization shows that it is composed of Quartz (66.2%) and Calcite (33.8%) (Figure 4C).

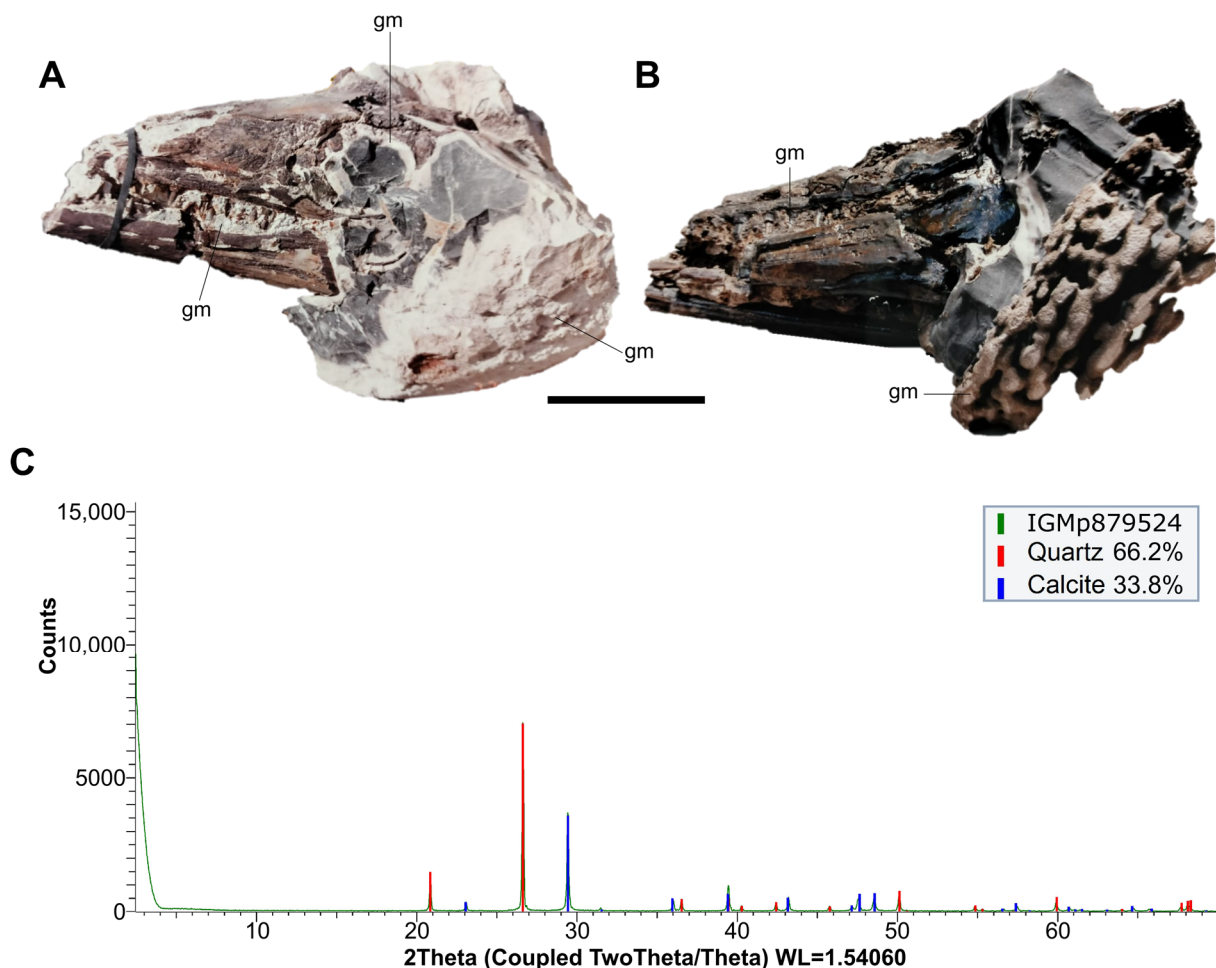


**Figure 4.** (A,B) Gray mineralization in the IGMp879524 skull. (A) Left lateral view of the skull within the concretion before acid preparation. (B) Left lateroventral view of the skull and concretion during chemical preparation. (C) Diffractogram of the gray mineralization; **Abbreviations:** gm, gray mineralization. Scale bar in (A,B): 10 cm.

Our petrographic observations of the thin sections indicated that the gray mineralization is mineralogically composed mainly of microcrystalline quartz (15  $\mu\text{m}$  approximately) and, in a smaller proportion, of microcrystalline calcite (micrite) randomly distributed

(Figure 5A). Some poorly preserved round structures resembling those of calcareous dinoflagellate cysts (following [23] (Figure 9C)) were identified in the gray mineralization (Figure 5D). The calcareous matrix of the concretion is mainly composed of micrite with a small proportion of pseudosparite and scattered clusters of microcrystalline quartz (Figure 5B). A few chloritized pseudosparite calcite crystals were found throughout both the gray mineralization and concretion. Thus, the main difference between the gray mineralization and the calcareous matrix is the amount of quartz (Figure 5C). The bone is composed of phosphate, and its pores are filled with sparitic calcite crystals (Figure 5E). Near the bone, there are small veins filled with microcrystalline quartz (Figure 5F).

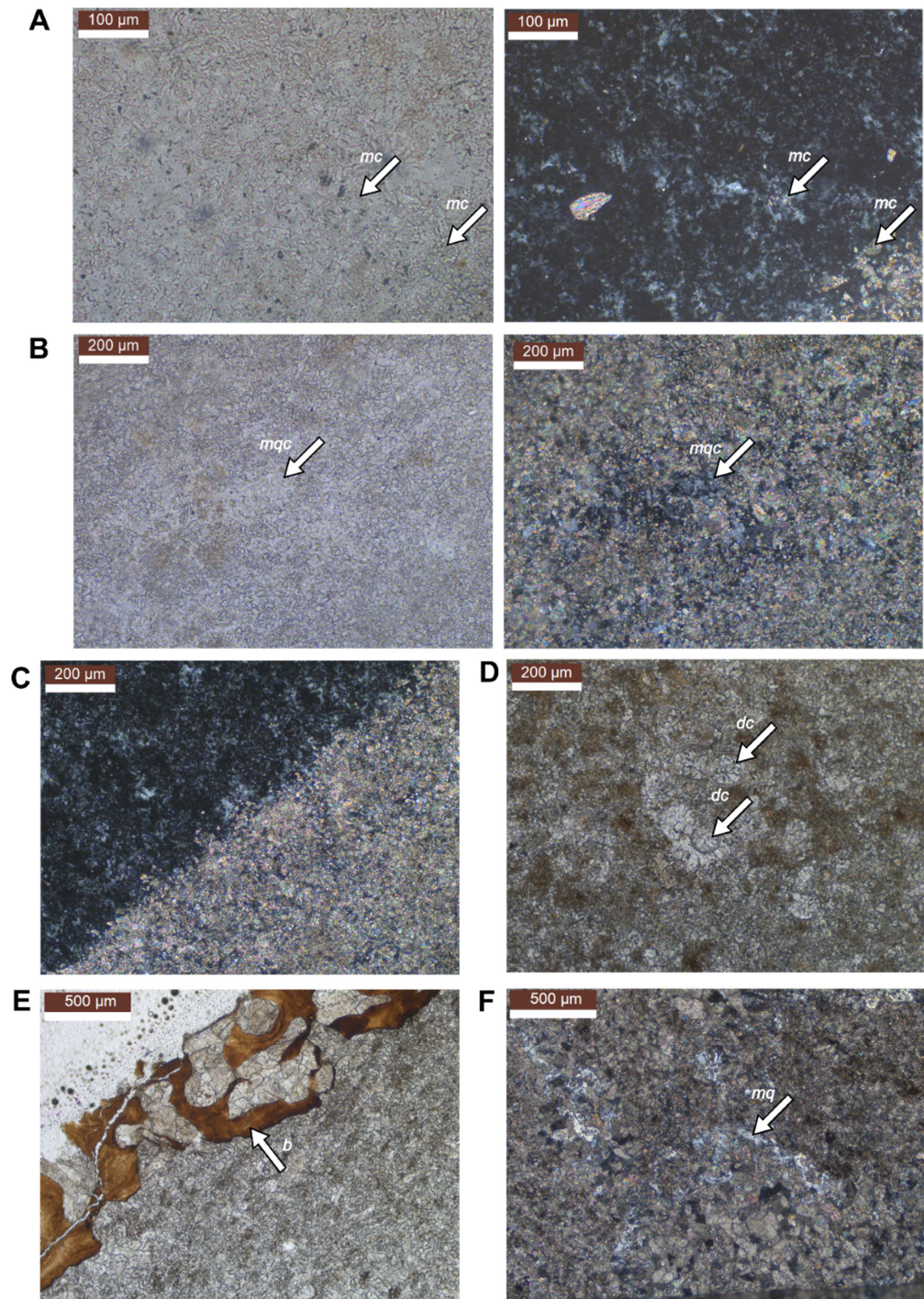


**Figure 5.** Thin section microphotographs. (A,B) With plane polarized light PPL (left) and crossed polarized light XPL (right). (A) Gray mineralization showing microcrystalline quartz with a smaller

proportion of microcrystalline calcite; (B) calcareous matrix showing microcrystalline calcite with scattered clusters of microcrystalline quartz. (C) Contact between the gray mineralization rich in quartz (left) and the matrix rich in calcite (right) (XPL). (D) Dinoflagellate cysts in the gray mineralization (PPL); (E) phosphatic bone with sparitic calcite crystals filling its pores (PPL). (F) Microcrystalline quartz filling veins in the calcareous matrix (XPL). **Abbreviations:** **b**, bone; **dc**, dinoflagellate cyst; **mc**, microcrystalline calcite; **m<sub>q</sub>**, microcrystalline quartz; **m<sub>qc</sub>**, microcrystalline quartz cluster.

In the Galembo Formation, where IGMp879524 comes from, the presence of beds and lenses of chert is frequent [13]. According to [24], silicification is found as a replacement feature in limestone sequences, usually as nodules and occasionally as beds. Trewin and Fayers [24] and Knauth [25] established that authigenic quartz is found abundantly in sedimentary rocks in the form of chert, commonly as granular microcrystalline quartz or microquartz (diameter generally less than 5–20  $\mu\text{m}$ ) that has replaced (silicified) pre-existing sediments such as carbonate, opal, or evaporite minerals. The presence of chert in the Galembo Formation and microcrystalline quartz and micrite in the gray mineralization and the concretion matrix of IGMp879524 suggests a partial silicification in the specimen IGMp879524 and an authigenic quartz replacing part of the calcite.

In the gray mineralization of the specimen, the silicification is around 60–70%, and in the concretion matrix, it is around 10–30%, showing a higher silicification in the gray mineralization than in the matrix surrounding the fossil. According to [24], the silicification process is promoted by a high concentration of carbonate ions, organic matter, and reduced pH; the silica is soluble in alkaline waters with a pH above 9, whereas calcite solubility increases with decreasing pH. Diagenetic waters undergoing a decrease in pH (acid) can be expected to dissolve calcite while silica precipitates, promoting the silicification of carbonates [24,25]. According to [25], the earliest stages of silicification in carbonate sequences occur in shell material, in which localized silica precipitation/carbonate dissolution are promoted by the bacterial breakdown of organic matter. This occurs because the decay of the organic matter (decaying tissues) contributes to the development of microenvironments, which geochemically differ in various ways from their immediate surroundings [26,27]. These microenvironments may form internally or externally of carcasses, and their geochemical conditions might promote the precipitation of minerals, such as silica [26,27]. Thus, selective silicification may result in scattered silicified fossils or fossil parts within limestone [24], as we found in our specimen. The scattered silicification in IGMp879524 indicates that there were spots of dissolution of calcite and precipitation of silica promoted by the formation of microenvironments with lower pH, probably associated with the bacterial breakdown of the non-biomineralized tissues. Nonetheless, microenvironment development only leads to mineral formation if the chemical species that precipitate in response to microbial metabolisms are present in sufficient supply [27]. Therefore, we can deduce that for silicification to occur, the concentration of dissolved silica in the diagenetic waters must be enough so it can precipitate and replace carbonates when the geochemical conditions are appropriate. The availability of silica in the environment during the deposition of the Galembo Formation is evidenced by the presence of beds of chert. The dinoflagellate cysts found in the gray mineralization suggests that the dissolution of dinoflagellate skeletons in the water could have been a source of silica.

Silicification in limestone sequences appears to be a relatively early diagenetic process, taking place during shallow burial [24,25]. The presence of silicification in the concretion containing IGMp879524 probably comes from the silicification of carbonates during early diagenesis. That is supported by the presence of calcite within the skull cavities, the gravity-displaced position of some bones in the skull, and the preservation of some chondrocranial cartilages, which indicate that the more labile cranial soft tissues were decaying during the diagenesis of the concretion. This decay process generated the acid microenvironments optimal for the dissolution of calcite and silicification.

## 6. Conclusions

In this study, we describe the exceptionally preserved chondrocranial elements found in a skull of a mosasaurid collected in north-central Colombia (specimen IGMp879524). We identified the interorbital septum, the planum suprasetale, parts of the trabeculae comunis, and remains in the position of the nasal septum and nasal capsules. The chondrocranium in IGMp879524 is greatly reduced, with the taeniae and pilae very poorly represented.

The chondrocranium of IGMp879524 has a narrow planum suprasetale that contacts the frontal, creating a narrow cavity for the olfactory tract. The well-preserved interorbital septum and absence of a fused pilae plate in IGMp879524 indicate that the optic muscle insertions were primarily inserted in the interorbital septum in this mosasaurid. Our results suggest that the chondrocranium in mosasaurids was reduced, more than in most lacertilians, including their closest recent relatives, the varanids. Nonetheless, this reduction was not as severe as that seen in snakes or amphisbaenians, which have extremely reduced chondrocranium and limbs. Although much information is still lacking, the new evidence presented in this contribution suggests that the reduction in chondrocranium in mosasaurids could be related to the modification of their limbs by adaptation to aquatic life.

We established that the concretion containing IGMp879524 suffered a partial and scattered silicification during early diagenesis, which allows the exceptional preservation of the chondrocranium. This silicification was possible by the supply of sufficient concentration of dissolved silica in the diagenetic waters during the formation of the concretion. We interpret that the silicification process was promoted by the formation of microenvironments with lower pH, associated with the bacterial breakdown of the non-biomineralized tissues of the skull.

**Author Contributions:** Conceptualization, M.E.P.-F., C.D.B.-C. and J.A.N.-R.; methodology, M.E.P.-F., C.D.B.-C. and J.A.N.-R.; software, C.F.Y.-L. and J.A.N.-R.; investigation, M.E.P.-F., C.D.B.-C. and J.A.N.-R.; writing—original draft preparation, M.E.P.-F., C.D.B.-C. and J.A.N.-R.; writing—review and editing, M.E.P.-F., C.D.B.-C. and J.A.N.-R.; visualization, C.F.Y.-L. and J.A.N.-R.; supervision, M.E.P.-F. All authors have read and agreed to the published version of the manuscript.

**Funding:** This research received no external funding.

**Institutional Review Board Statement:** Not applicable.

**Data Availability Statement:** The data that support the findings of this study are available from the corresponding author upon reasonable request.

**Acknowledgments:** We are grateful to the Museo Geológico Nacional José Royo y Gómez for granting access to the specimen under their care. The SHAI0 CLINIC research group provided the CT scan. We want to thank Ricardo Buitrago, Marco Chala, and Juliana Morantes, members of the SHAI0 research group, for all their assistance during the scanning of the specimen. We would like to thank CT scan technicians Martin Meneses and Julio Quiroga from the Clinica SHAI0 for their collaboration in the scanning process. Furthermore, we thank the Lithochemical Characterization Laboratory of the Departamento de Geociencias of the Universidad Nacional de Colombia for allowing us to run the XRD analysis. We also want to thank Carlos Rodríguez Esquivel for his assistance in the XRD analysis. Likewise, we would like to thank Hernán Ortiz from the Vertebrate Paleontology Laboratory and Armando Sanchez from the Petrographic Techniques Laboratory of the Departamento de Geociencias of the Universidad Nacional de Colombia for their assistance in the elaboration of the thin sections. We would like to thank Diana Montoya for their useful comments on the elements seen in the thin sections. We are indebted to Ingmar Werneburg for sharing essential bibliography. Likewise, we are grateful to the two anonymous reviewers whose comments help to improve the final version of this manuscript.

**Conflicts of Interest:** The authors declare no conflicts of interest.

## References

1. De Beer, G.R. The early development of the chondrocranium of the lizard. *Q. J. Microsc. Sci.* **1930**, *73*, 707–739.
2. Bellairs, A.D.; Kamal, A.M. The chondrocranium and the development of the skull in recent reptiles. In *Biology of the Reptilia, Volume 11, Morphology F*; Gans, C., Parsons, T.S., Eds.; Academic Press: New York, NY, USA, 1981; Volume 11, pp. 1–283.

3. Jones, M.E.; Gröning, F.; Aspden, R.M.; Dutel, H.; Sharp, A.; Moazen, M.; Fagan, M.J.; Evans, S.E. The biomechanical role of the chondrocranium and the material properties of cartilage. *Vertebr. Zool.* **2020**, *70*, 699–715. [[CrossRef](#)]
4. Kardong, K. *Comparative Anatomy, Function, Evolution*, 8th ed.; Mc Graw Hill: New York, NY, USA, 2019; pp. 1–814.
5. Bellairs, A.D. The anterior brain-case and interorbital septum of Sauropsida, with a consideration of the origin of snakes. *Zool. J. Linn. Soc.* **1949**, *41*, 485–512. [[CrossRef](#)]
6. Shrivastava, R.K. The structure and development of the chondrocranium of Varanus. Part I. The development of the ethmoidal region. *Okajima Folia Anat. Jpn.* **1963**, *39*, 55–83. [[CrossRef](#)] [[PubMed](#)]
7. Shrivastava, R.K. The structure and development of the chondrocranium of Varanus. Part II. The development of the orbito-temporal region. *J. Morphol.* **1964**, *115*, 97–108. [[CrossRef](#)]
8. Shrivastava, R.K. The structure and development of the chondrocranium of Varanus. Part III. The otic and occipital regions, basal plate, viscerocranium, and certain features of the osteocranium. *Morphol. Jahrb.* **1964**, *106*, 147–187.
9. Yaryhin, O.; Werneburg, I. The origin of orbitotemporal diversity in lepidosaurs: Insights from tuatara chondrocranial anatomy. *Vertebr. Zool.* **2020**, *69*, 169–181. [[CrossRef](#)]
10. Camp, C.L. *California Mosasaurs*; Memoirs of the University of California; University of California Press: Berkeley, CA, USA, 1942; Volume 13, pp. 1–68.
11. Russel, D. Systematics and morphology of American mosasaurs (Reptilia, Sauria). *Bull. Peabody Mus. Nat. Hist.* **1967**, *23*, 1–241.
12. Páramo-Fonseca, M.E. Mosasauroids from Colombia. *Bull. Soc. Geol. Fr.* **2012**, *183*, 103–109. [[CrossRef](#)]
13. Terraza-Melo, R. “Formación La Luna”: Expresión espuria en la geología colombiana. In *Estudios Geológicos y Paleontológicos Sobre el Cretácico en la Región del Embalse del río Sogamoso, Valle Medio del Magdalena*, 1st ed.; Etayo-Serna, F., Ed.; Servicio Geológico Colombiano: Bogotá, Colombia, 2019; Compilación de los Estudios Geológicos Oficiales en Colombia Volume XXIII; pp. 303–362.
14. Morales, L.G.; Podesta, D.J.; Hatfield, W.C.; Tanner, H.; Jones, S.H.; Barker, M.H.S.; O’Donoghue, D.J.; Mohler, C.E.; Dubois, E.P.; Jacobs, C.; et al. General Geology and oil occurrence of Middle Magdalena Valley, Colombia. In *Habitat of Oil*; American Association of Petroleum Geologist: Tulsa, OK, USA, 1958.
15. Thorez, J. *Practical Identification of Clay Minerals*; Institute of Mineralogy—Liege State University: Liege, Belgium, 1976; pp. 1–90.
16. Bonilla, G.; Sarmiento, G.A.; Gaviria, S. Proveniencia y transformación diagenética de minerales arcillosos del Maastrichtiano—Paleoceno al norte de Bogotá, Cordillera Oriental de Colombia. *Geol. Column* **2011**, *36*, 179–195.
17. Bellairs, A.D. Observations on the snout of Varanus, and a comparison with that of other lizards and snakes. *J. Anat.* **1949**, *83*, 116–146. [[PubMed](#)]
18. Konishi, T. A mosasaur (Squamata: Mosasauridae) sneeze: A hypothesis concerning salt excretion in the top predators of the Cretaceous Seas. In Proceedings of the 75th Annual Meeting of the Society of Vertebrate Paleontology, Dallas, TX, USA, 14–17 October 2015; MacKenzie, A., Maxwell, E., Miller-Camp, J., Eds.; 2015.
19. Yaryhin, O.; Werneburg, I. Tracing the developmental origin of a lizard skull: Chondrocranial architecture, heterochrony, and variation in lacertids. *J. Morphol.* **2018**, *279*, 1058–1087. [[CrossRef](#)] [[PubMed](#)]
20. Jones, M.E.; Gröning, F.; Dutel, H.; Sharp, A.; Fagan, M.J.; Evans, S.E. The biomechanical role of the chondrocranium and sutures in a lizard cranium. *J. R. Soc. Interface* **2017**, *14*, 20170637. [[CrossRef](#)] [[PubMed](#)]
21. Zhang, Z.; Yaryhin, O.; Koyabu, D.; Werneburg, I. Morphological association between muscle attachments and ossification sites in the late cartilaginous skull of tuatara embryos. *J. Morphol.* **2022**, *283*, 908–931. [[CrossRef](#)] [[PubMed](#)]
22. Yaryhin, O.; Klembara, J.; Pichugin, Y.; Kaucka, M.; Werneburg, I. Limb reduction in squamate reptiles correlates with the reduction of the chondrocranium: A case study on serpentiform anguids. *Dev. Dyn.* **2021**, *250*, 1300–1317. [[CrossRef](#)] [[PubMed](#)]
23. Montoya Arenas, D.M. Formación La Paja: Descripción de la sección tipo. Influencia de los tapices microbiales en su génesis. In *Estudios Geológicos y Paleontológicos Sobre el Cretácico en la Región del Embalse del Río Sogamoso, Valle Medio del Magdalena*, 1st ed.; Etayo-Serna, F., Ed.; Servicio Geológico Colombiano: Bogotá, Colombia, 2019; Compilación de los Estudios Geológicos Oficiales en Colombia Volume XXIII; pp. 55–156.
24. Trewin, N.H.; Fayars, S.R. Sedimentary Rocks | Chert. In *Encyclopedia of Geology*; Richard, C., Selley, L., Cocks, M., Ian, R., Palmer, R., Eds.; Elsevier: Amsterdam, The Netherlands, 2007; Volume 3, pp. 154–196. [[CrossRef](#)]
25. Knauth, L.P. Chapter 7. Petrogenesis of Chert. In *Silica: Physical Behavior, Geochemistry, and Materials Applications*, 1st ed.; Heaney, P., Prewit, C., Gibbs, G., Eds.; De Gruyter: Berlin, Germany, 1994; pp. 233–258. [[CrossRef](#)]
26. McNamara, M.E.; Orr, P.J.; Kearns, S.L.; Alcalá, L.; Anadón, P.; Penalver Molla, E. Soft tissue preservation in Miocene frogs from Libros, Spain: Insights into the genesis of decay microenvironments. *PALAIOS* **2009**, *24*, 107–117. [[CrossRef](#)]
27. Muscente, A.D.; Schiffbauer, J.D.; Broce, J.; Laflamme, M.; O’Donnell, K.; Boag, T.H.; Meyer, M.; Hawkins, A.D.; Huntley, J.W.; McNamara, M.; et al. Exceptionally preserved fossil assemblages through geologic time and space. *Gondwana Res.* **2017**, *48*, 164–188. [[CrossRef](#)]

**Disclaimer/Publisher’s Note:** The statements, opinions and data contained in all publications are solely those of the individual author(s) and contributor(s) and not of MDPI and/or the editor(s). MDPI and/or the editor(s) disclaim responsibility for any injury to people or property resulting from any ideas, methods, instructions or products referred to in the content.